Z. Phys. D 37, 241–247 (1996)

ZEITSCHRIFT
FÜR PHYSIK D

Energy pooling in cesium vapor

C. Vadla[1], **K. Niemax**[2], **J. Brust**[2]

[1] Institute of Physics of the University, Bijenicka 46, 10000 Zagreb, Croatia
[2] Institut für Physik, Universität Hohenheim, Garbenstrasse 30, D-70599 Stuttgart, Germany

Received: 22 December 1995/Final version: 31 January 1996

Abstract. We report an experimental study of energy pooling collisions involving Cs atoms in the 6*P* and 5*D* states. The 5*D* state was populated by a *cw* dye-laser tuned to the cesium dipole-forbidden transition $6S \rightarrow 5D$ at 685.0 nm. The 6*P* state was populated by subsequent radiative relaxation of the 5*D* state. The 6*P* population density was determined from the absorption of a *cw* diode-laser probe beam. The population densities of the 5*D* state and the higher, by energy pooling excited states were determined by measuring the corresponding fluorescence intensities relative to the fluorescence intensity from the optically thin quasi-static wings of the cesium D_2 line. The rate coefficient for the process $Cs^*(6P) + Cs^*(6P) \rightarrow Cs^{**}(6D) + Cs(6S)$ is found to be $(4.2 \pm 0.13) \times 10^{-10}\,cm^3\,s^{-1}$ at $T = 570\,K$. In addition, estimates of the rate coefficients for the processes $Cs^*(6P) + Cs^*(5D) \rightarrow Cs^{**}(7D) + Cs(6S)$ and $Cs^*(5D) + Cs^*(5D) \rightarrow Cs^{**}(7F) + Cs(6S)$ are given.

PACS: 34.50; 32.00

1 Introduction

During the last three decades, the electronic excitation energy transfer in low-energy atomic collisions has been the subject of many experimental and theoretical investigations. Most of these studies were concerned with the collisions involving one excited and one ground-state atom, for example, level mixing and quenching. More recently there has been substantial interest in collisions of two excited atoms which produce one highly excited atom and one atom in the ground state. The first observation of such a process, lately named as "energy pooling", has been reported by Klyucharev and Lazarenko [1], who studied the fluorescence spectrum of cesium vapor in a cell irradiated with the light from a cesium gas-discharge lamp. It was found that the population density of the Cs 6*P* state decreases with increasing cesium ground-state number density, while the population density of the Cs 6*D* state increases simultaneously. The authors in [1] concluded that this effect is due to collisional excitation transfer process $Cs^*(6P) + Cs^*(6P) \rightarrow Cs^{**}(6D) + Cs(6S)$ and estimated an upper limit of $10^{-13}\,cm^2$ for the cross section of this reaction.

The application of laser techniques to the field [2] confirmed the existence of energy pooling (EP) processes and enabled more precise experiments. In subsequent quantitative studies the most investigated EP processes were the collisions involving two homonuclear [3–5] or heteronuclear [6, 7] alkali atoms excited to their first resonance states, since from the experimental as well as from the theoretical point of view, alkali atoms are the most convenient to study electron, i.e. excitation energy transfer processes. However, in recent years the investigations of EP processes were extended to atoms with two outer electrons [8, 9].

In the present paper an investigation of the following EP processes in a cesium vapor is reported:

$$Cs^*(6P) + Cs^*(6P) \rightarrow Cs^{**}(6D) + Cs(6S), \quad (1)$$

$$Cs^*(6P) + Cs^*(5D) \rightarrow Cs^{**}(7D) + Cs(6S), \quad (2)$$

and

$$Cs^*(5D) + Cs^*(5D) \rightarrow Cs^{**}(7F) + Cs(6S). \quad (3)$$

The process (1), studied experimentally in the pioneering work [1], has been treated also theoretically about twenty years ago [10]. To our knowledge, the second and the third of these processes which involve the 5*D* states have not been reported yet. Moreover, this is the first study of EP processes involving alkali atoms in excited states which are higher than the resonance state.

The measurements were performed in the steady-state regime. In this case, and in the absence of population and depopulation processes other than EP and radiative relaxation, the population density $N(p)$ of the final highly excited state obeys the following steady-state rate equation:

$$\frac{d}{dt} N(p) = 0 = K_p N(m) N(n) - N(p)/\tau_p. \quad (4)$$

Here, K_p is the EP rate coefficient, m and n denote initial states, and τ_p is the radiative lifetime of the final highly excited state p. The determination of the absolute value of K_p requires the measurement of the number densities of all states involved. As usual in EP esperiments, the determination of the number densities of the excited atoms was performed by the measurement of the relevant fluorescence line intensities. In typical EP experiments the atoms are excited to the first resonance states by laser radiation and the detectable EP fluorescence lines appear if the number densities of the ground-state atoms are at least of the order of 10^{11} cm^{-3}. At these densities self-absorption and radiative trapping of the resonance lines become significant and make a quantitative analysis very difficult. These effects are the main sources of errors in evaluation of the EP rate coefficients.

In this work we applied a method which circumvented the problem of the radiative trapping of the resonance lines. Our approach, which is described in the following paragraph, is based on accurate knowledge of the quasi-static line profiles of the alkali D lines. The fluorescence of the alkali resonance line wings was used as a quasi-continuous, relative standard of radiation. This method is especially convenient for measurements at higher atom number densities, i.e. it provides the values for EP rate coefficients at higher temperatures than in previous experiments.

2 Method

Generally, when resonance broadening is dominant, the absorption coefficient in the quasi-static wing of the resonance line is given by the following expression [11]:

$$\kappa_{ij}(\nu) = \frac{4\pi^2 e^2}{3mc} f_{ij} C_3 \frac{N^2(i)}{(\nu - \nu_{ij})^2}. \tag{5}$$

Here, C_3 is the effective resonance interaction constant for the $i \to j$ transition, $N(i)$ is the ground-state number density, f_{ij} is the oscillator strength and ν_{ij} is the central frequency. As shown in [12], equation (5) holds for the outer wings of the alkali first resonance doublets, i.e. for the blue wings of the D_2 and for the red wings of the alkali D_1 lines. It is valid with an accuracy better than 5% if the detuning $\Delta\nu = \nu - \nu_{ij}$ is smaller than one third of the fine-structure splitting. The calculated values for C_3 constants reported in [12] are in excellent agreement with the experimental results of Horvatic et al. [13]. According to these investigations the resonance interaction constants for cesium are $C_3(6P_{1/2}) = 3.4 \times 10^{-9}$ cm^2 s^{-1} and $C_3(6P_{3/2}) = 5.0 \times 10^{-9}$ cm^3 s^{-1}, respectively. The absorption coefficient in the outer quasi-static wings of the alkali first resonance doublets $n_oS_{1/2} \to n_oP_J$ can be written as:

$$\kappa_J(\nu) = \alpha_J \frac{N^2(n_oS)}{(\Delta\nu)^2}, \tag{6}$$

where, in case of cesium ($n_0 = 6$, $J = 1/2$, $3/2$), $\alpha_{1/2} = 1.3 \times 10^{-10}$ cm^5 s^{-2} and $\alpha_{3/2} = 3.9 \times 10^{-10}$ cm^5 s^{-2}.

The absorption coefficient $\kappa_{ij}(\nu)$ is related to the spectral emission coefficient $A^{\nu}_{ji}(\nu)$ via well known relation:

$$\kappa_{ij}(\nu) = N(i) \frac{g_j}{g_i} \frac{\lambda_{ij}^2}{8\pi} A^{\nu}_{ji}(\nu), \tag{7}$$

where g_i and g_j are the statistical weights of the states i and j, respectively.

The combination of (5) and (7) yields the expression for the spectral emission coefficient in the resonance quasi-static wing:

$$A^{\nu}_{ij}(\nu) = \frac{32\pi^3 e^2}{3\lambda_{ij}^2 mc} \frac{g_i}{g_j} f_{ij} C_3 \frac{N(i)}{(\nu - \nu_{ij})^2}. \tag{8}$$

For alkali resonance lines, analogously to equation (6), we may write

$$A^{\nu}_J(\nu) = \beta_J \frac{N(n_oS)}{(\Delta\nu)^2}, \tag{9}$$

where the factors β for cesium are $\beta_{1/2} = 0.40$ cm^3 s^{-2} and $\beta_{3/2} = 0.67$ cm^3 s^{-2}.

The spectral intensity of the optically thin quasi-static wings of the resonance lines emitted from the infinitesimal volume dV is given by:

$$dI^{\nu}_J(\Delta\nu) = h\nu_J N(n_oP_J) A^{\nu}_J(\nu)\, dV. \tag{10}$$

The intensity of the emitted radiation is spectrally integrated over the frequencies within the band-pass $\delta\nu$ of the detection system and averaged over the observed volume. If the band-pass $\delta\nu$ is small compared with the detuning from the line center $\Delta\nu$, the spectral intensity of the line wing can be regarded as constant within the interval $(\nu, \nu + \delta\nu)$. In this case, assuming the number densities in expressions (9) and (10) to be functions of the space coordinates $\boldsymbol{r}$, the measured intensity in the resonance wing can be described as follows:

$$I_J(\Delta\nu) \propto h\nu_J \beta_J \frac{\delta\nu}{(\Delta\nu)^2} \int d^3\boldsymbol{r} N(n_0S, \boldsymbol{r}) N(n_0P_J, \boldsymbol{r}). \tag{11}$$

On the other hand, if the monochromator band-pass is large in comparison with the width of an optically thin line arising in a $p \to p'$ transition, the detected line intensity is spectrally integrated over the frequencies within the whole line profile. Denoting the total transition probability by $A_{pp'}$, and the spatial distribution of the population in the upper level with $N(p, \boldsymbol{r})$, we may express the measured intensity of such a line as:

$$I_{pp'} \propto h\nu_{pp'} A_{pp'} \int d^3\boldsymbol{r} N(p, \boldsymbol{r}). \tag{12}$$

Next, we apply the above expressions in order to evaluate the rate coefficients for an EP process involving two alkali atoms excited in the first resonance state:

$$X^*(n_oP) + X^*(n_oP) \to X(n_oS) + X^{**}(p). \tag{13}$$

We assume an isotropic ground-state number density $N(n_oS)$ and an optical excitation of the atoms by an axially symmetric laser beam. In this case, the spatial distributions of the excited atoms, governed by the shape of the laser beam, are only radially dependent. Accordingly, the population densities of the excited atoms can be

represented in the form $N = N_0 f(r)$, where N_0 is the population density at the laser beam axis and $f(r)$ is a distribution function normalized to unity at $r = 0$. The corresponding rate equation for the population density of the state p is given by:

$$N_0(p) f(p, r)/\tau_p = K_p N_0^2(n_o P) f^2(n_o P, r). \tag{14}$$

Here, the $f(p, r)$ and the $f(n_0 P, r)$ denote the distribution function of the atoms in the state p and the resonance state, respectively.

Applied to $r = 0$, (14) yields the solution for K_p:

$$K_p = \frac{N_0(p)}{\tau_p N_0^2(n_o P)}, \tag{15}$$

which consequently gives the relation between the distribution functions:

$$f(p, r) = f^2(n_o P, r). \tag{16}$$

By combination of (11), (12) and (16) one obtains the expression for the population density of the EP state p in the centre of the excitation zone:

$$N_0(p) = \frac{v_J}{v_{pp'}} \frac{\beta_J \delta v}{(\Delta v)^2 \tau_p A_{pp'}} \frac{I_{pp'}}{I_J(\Delta v)} N(n_o S) N_0(n_o P_J) \times \frac{\int r^2 \, \mathrm{d}r \, f(n_o P_J, r)}{\int r^2 \, \mathrm{d}r \, f^2(n_o P_J, r)}. \tag{17}$$

The relative population density of the state p with respect to the population density in the fine-structure sublevel $n_o P_J$ of the first alkali resonance state can be derived from (17) if $I_{pp'}/I_J(\Delta v)$, the number density of the ground-state atoms and spatial distribution of the $n_o P_J$ state are measured. In order to determine the absolute value for the population density in the p state, the number density $N_0(n_o P_J)$ has to be measured too.

We introduce the ratio $\xi = N_0(n_o P_{J'})/N(n_o P_J)$ of the fine structure ($J = 3/2$, $J' = 1/2$) sublevels population densities. Using this substitute and expression (17), one obtains equation (15) in the following form:

$$K_p = \frac{v_J}{v_{pp'}} \frac{\beta_J \delta v}{(\Delta v)^2 \tau_p A_{pp'}} \frac{I_{pp'}}{I_J(\Delta v)} \frac{N(n_o S)}{(1 + \xi)^2 N_0(n_o P_J)} \times \frac{\int r^2 \, \mathrm{d}r \, f(n_o P, r)}{\int r^2 \, \mathrm{d}r \, f^2(n_o P, r)}. \tag{18}$$

The EP rate coefficient K_p can be evaluated from the above equation if the relative intensities $I_{pp'}/I_J(\Delta v)$, the ground state number density and the population densities in the $n_o P_J$ states are measured. The spatial distributions of the $n_o P_J$ states are assumed to be equal. If they are not equal, the evaluation of K_p is more complicated. Namely, the rate coefficient K_p is defined as total rate coefficient, which comprises three particular EP contributions:

$$K_p N_0^2(n_o P) = K_p(\tfrac{1}{2}, \tfrac{1}{2}) N_0^2(n_o P_{1/2}) + K_p(\tfrac{1}{2}, \tfrac{3}{2}) N_0(n_o P_{1/2}) N_0(n_o P_{3/2}) + K_p(\tfrac{3}{2}, \tfrac{3}{2}) N_0^2(n_o P_{3/2}), \tag{19}$$

and each particular spatial distribution should be taken into account.

3 Experiment and measurements

The experimental arrangement was similar to that, which has been described in a recent publication [14]. The cesium vapor was generated in the middle part of a T-shaped stainless-steel heat-pipe with argon as a buffer gas ($p = 1$ mbar). The cesium ground-state number density was determined by a white light absorption measurement of the absorption coefficient in the blue quasi-static wing of the self-broadened Cs D_2 line [13]. The measurements were performed in a narrow Cs density range ($0.95 \times 10^{16}\,\mathrm{cm}^{-3}$ and $1.05 \times 10^{16}\,\mathrm{cm}^{-3}$) and, according to [15], the corresponding temperature was about 570 K. Cesium ground-state atoms were directly excited to the $5D_{5/2}$ state by a *cw* single-mode, frequency stabilized ring dye-laser (dye: DCM). The frequency of the dye laser was tuned to the centre of the stronger hyperfine component of the "forbidden" transition $6S_{1/2} \rightarrow 5D_{5/2}$ (wavelength: 685.0 nm). The pump laser beam had a Gaussian shape (full width ≈ 2 mm) and a power of 30 mW.

The $5D_{3/2}$ state was excited by collisional fine-structure mixing from the $5D_{5/2}$ state, while cesium atoms in the $6P_J$ states were produced by radiative relaxation processes $5D_J \rightarrow 6P_J$ (see Fig. 1). The population density in the Cs $6P_{3/2}$ state was measured by laser absorption and fluorescence using a single-mode, frequency stabilized diode laser (Hitachi HL 7851, power: 50 mW). The diode-laser probe beam was aligned along the axis of the dye laser pump beam and its frequency was scanned across the $6P_{3/2} \rightarrow 8S_{1/2}$ transition at 794.6 nm. The width of the probe beam was less than 0.5 mm and, in order to avoid optical saturation, its power was reduced to about 50 μW. The absorption of the pump and probe beams in the cesium vapour column was measured by the photodiodes. For cesium ground-state number densities of about $10^{16}\,\mathrm{cm}^{-3}$ the attenuation of the pump beam after pasing the vapour column (length: 5 cm) was about 30%.

The fluorescence from the excited vapour was observed perpendicularly to the laser beam direction. The central part of the fluorescence zone (length: 5 mm) was imaged parallel to the entrance slit of a 1 m McPherson monochromator and the signals were detected by a RCA 20 multiplier. With a slit-widths of 100 μm the corresponding monochromator band-pass was 0.082 nm (2.9×10^{10} Hz) at the wavelength of the cesium D lines. Together with the fluorescence at the wavelengths of the resonant and "forbidden" Cs lines, we observed optically thin EP lines belonging to the sharp ($nS_{1/2} \rightarrow 6P_J$), diffuse ($nD_J \rightarrow 6P_J$), and Bergman ($nF_J \rightarrow 5D_J$) series. A partial fluorescence spectrum obtained by scanning the monochromator is shown in Fig. 2a. The signals recorded by tuning the probe laser over the $6P_{3/2} \rightarrow 8S_{1/2}$ transition are displayed in Fig. 2b. We note that the typical line widths of the measured optically thin lines were more than ten times smaller than the monochromator band-pass (see Fig. 2b). On the other hand, the quasi-static wing intensity was measured for typical detunings of 2×10^{12} Hz (5 nm), which means that the conditions for the application of our approach, regarding the monochromator band-pass as defined in Sect. 2, were completely fulfilled.

The fluorescence zone was imaged in 1 : 2 ratio onto the entrance slit of the monochromator and only the

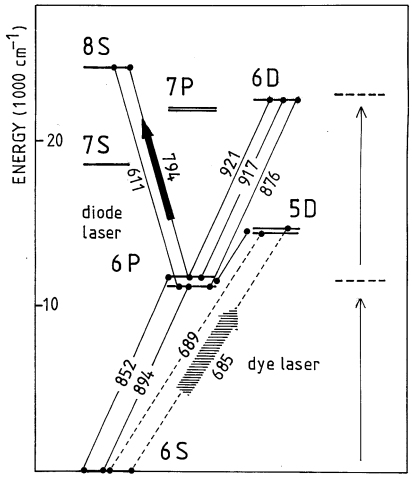

Fig. 1. Partial term diagram of cesium including the laser excitation and the probe transitions. The wavelengths of the relevant radiative transitions are given in nm

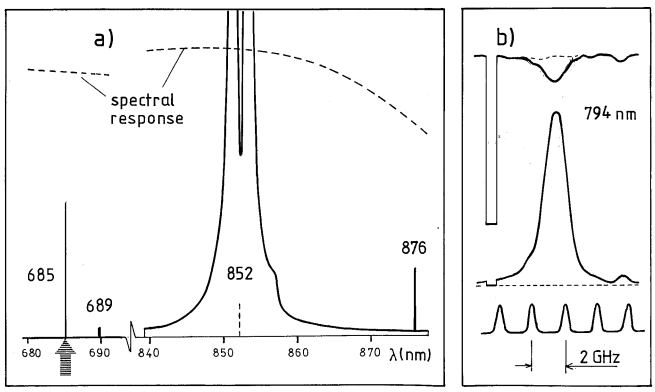

Fig. 2. a Partial emission spectrum of cesium comprising the strong EP line. The spectrum is recorded at a cesium number density of 0.95×10^{16} cm^{-3}. The population densities in the $6P$ and $5D$ states were 2.9×10^{11} cm^{-3} and 5×10^{10} cm^{-3}, respectively. **b** Simultaneously recorded absorption (*upper trace*) and the fluorescence (*middle trace*) spectra of the probe line at 794.6 nm, obtained by scanning the diode laser. Spectrum dispersion marks (*lower trace*) are the transmission peaks of a 150 MHz confocal Fabry-Perot interferometer

radiation from a thin layer parallel to the beam axis was measured (see Fig. 3a). In order to get the information about the spatial distribution of the excited cesium atoms, the position r of the observed layer within the axially symmetric fluorescence zone was changed by moving the imaging lens in y direction. The intensity distributions measured at three wavelengths are displayed in Fig. 3b. The intensity of the sensitized "forbidden" line at 689.6 nm represents the power distribution of the pump-laser beam. The intensity of the optically thin resonance line wing represents the distribution $N(6P)$ of the cesium atoms in the first resonant states. Due to the radiation trapping and diffusion, this distribution is broader than that of the 689.6 nm line. The intensity of the 876.3 nm line, as expected for an EP line, indicates the quadratic dependence of the population density of the $6D$ state with respect to

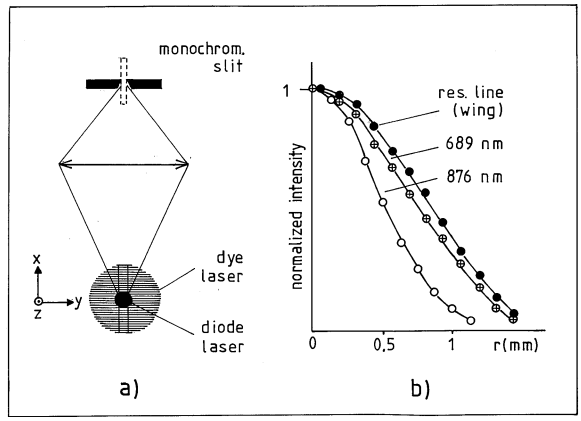

Fig. 3. a Imaging of the fluorescence zone onto the monochromator entrance slit (not in scale). For further explanations, see text. **b** Spatial distributions of the fluorescence intensities of the optically thin D_2 line wing, the quadrupole line at 689 nm and the EP line at 876 nm, obtained by translation of the imaging lens

the spatial density distribution of the $6P$ state. No difference between the spatial distributions of D_1 and D_2 line wing intensities was observed.

The populatin density of the Cs $6P_{1/2}$ state was determined by measurement of the D_1 to D_2 line wing intensities ratio. The obtained value for $N(6P_{1/2})/N(6P_{3/2})$ was 1.6, which is lower than expected (1.9) for thermal equilibrium at the experimental temperature. The population density of the $5D_{3/2}$ was evaluated from the ratio between the intensity of the sensitized "forbidden" 689.6 nm line and the intensity of the resonance line wing, by using the expressions (11) and (12). The population density of the $5D_{5/2}$ state was not directly measured because the fluorescence of the 685.0 nm line was blended by scatter of the pump laser radiation. For the determination of $N_0(5D_{5/2})$ we used the rate equation for population density of the collisionally populated $5D_{3/2}$ state. This simple rate equation includes the radiative relaxation of the $5D_{3/2}$ state and the mixing rates G and H for $5D_{5/2} \rightarrow 5D_{3/2}$ and $5D_{3/2} \rightarrow 5D_{5/2}$ collisional transitions, respectively. Since the heat-pipe was running near the heat-pipe mode, the mixing was predominantly due to collisions with cesium ground-state atoms, while the influence of the collisions with buffer gas atoms was negligible. The value of the corresponding cross section $\sigma_G = 7 \times 10^{-15}$ cm^2 was taken from [16] and σ_H was calculated using the principle of detailed balancing. Taking into account the cesium number density 1×10^{16} cm^{-3}, the mean Maxwellian relative velocity 4.4×10^4 cm s^{-1}, and the radiative life time of the $5D_{3/2}$ state ($\tau = 1.4 \times 10^{-6}$ s) given in [17], we obtained $N(5D_{5/2})/N(5D_{3/2}) = 1.25$. In thermal equilibrium this value should be 1.5.

In order to change the excited state populations, the power of the pump laser beam was varied by the neutral density filters. The measurements were made at five different population densities of the $6P_{3/2}$ state between 5×10^{10} cm^{-3} and 2.2×10^{11} cm^{-3}. The corresponding population density of the $5D_{3/2}$ state was between 1×10^{10} cm^{-3} and 4.4×10^{10} cm^{-3}.

The population densities of the higher S, D and F cesium states were calculated from the measured

fluorescence intensities $I_{pp'}$ of EP lines relative to the wing intensity $I_{3/2}(\Delta\nu)$ of the D_2 line via (17). Here we used the theoretical transition probabilities taken from [17]. Even at the highest population densities of the $6P$ and $5D$ states, all transitions from highly excited states were optically thin. For instance, the intensities of the 876.3 nm and 921.1 nm lines arising from the $6D_{3/2} \rightarrow 6P_{1/2,3/2}$ transition were found to be in the ratio 5:1, which is close to the ratio of their transition probabilities (4.8:1). An additional check was made by calculation of the optical depths of the lines under consideration. Assuming the lines to be only broadened by the Doppler effect, the calculated maximal optical depths $\kappa(\nu_0)d$ for the side-on observed fluorescence zone of diameter $d \approx 1$ mm were about 0.2 for the strongest transitions.

The population densities of the higher P states could not be determined because the fluorescence of the $nP_J \rightarrow 6S_{1/2}$ lines showed self-absorption and the $nP_J \rightarrow 5D_J$ lines were too weak. The schematic representation of the relative population densities obtained from the measurement at number densities $N_0(6P) = N_0(6P_{3/2}) + N_0(6P_{1/2}) = 2.9 \times 10^{11}\ \mathrm{cm}^{-3}$ and $N_0(5D) = N_0(5D_{5/2}) + N_0(5D_{3/2}) = 5 \times 10^{11}\ \mathrm{cm}^{-3}$ are displayed in Fig. 4. As one can conclude from this figure, relatively high populations of the $6D$, $7D$ and $7F$ states are generated by EP collisions in the systems Cs*($6P$) + Cs*($6P$), Cs*($6P$) + Cs*($5D$) and Cs*($5D$) + Cs*($5D$), respectively. The population densities of S states are low, which indicates very weak EP and collisional mixing effects.

4 Analysis and results

EP has been observed by using relatively low-power laser excitation. The maximum pump power density applied was about $3\mathrm{W/cm}^2$ and the maximum pump rate achieved at the $6S_{1/2} \rightarrow 5D_{5/2}$ quadrupole transition was about $10^2\ \mathrm{s}^{-1}$. In this way, less than 0.01% of the cesium atoms were transferred to excited states. Under these conditions, the ionisation and the ion-electron recombination are negligible and the populations of the higher states are primarily produced by EP collisions. However, owing to the relatively high density of cesium ground-state atoms, level mixing effects are expected to be significant.

4.1 The 6D state

The population of the $6D$ state is governed by the EP process Cs*($6P$) + Cs*($6P$) → Cs*($6D$) + Cs($6S$), and in addition, by the radiative relaxation of the higher-lying P and F states. In the steady-state regime the corresponding rate equation is:

$$\frac{\mathrm{d}}{\mathrm{d}t} N(6D) = 0 = -N(6D)/\tau_{6D} + K_{6D} N^2(6P) + \sum A_{nF6D} N(nF) + \sum A_{nP6D} N(nP). \qquad (20)$$

Here, K_{6D} is the rate coefficient for the process (1). Using calculated values for lifetimes and transition probabilities in cesium [17], we estimated the values for A_{nF6D} to be of the order of about $5 \times 10^5\ \mathrm{s}^{-1}$. Regarding the value for

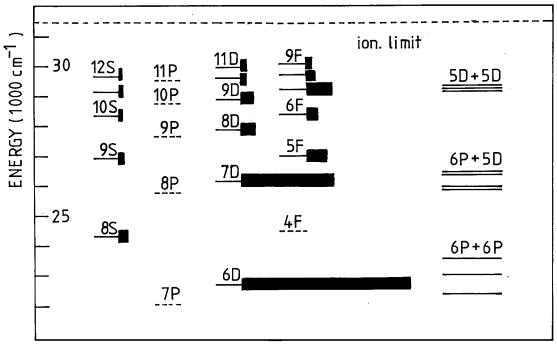

Fig. 4. Relative population densities of the highly excited cesium states in the centre of the excitation zone. The lengths of the broad bars represent the values of the number densities. In particular, $N_0(6D) = 2.1 \times 10^6\ \mathrm{cm}^{-3}$. The data are obtained at population densities $N_0(6P) = 2.9 \times 10^{11}\ \mathrm{cm}^{-3}$ and $N_0(5D) = 5 \times 10^{10}\ \mathrm{cm}^{-3}$

$\tau_{6D} = 6 \times 10^{-8}$ s [17] and the data displayed in Fig. 4, it is easy to show that the sum $\Sigma A_{nF6D} N(nF)$ is about 50 times smaller than $N(6D)/\tau_{6D}$. Similarly, we estimate the radiative contributions from the nP states to be also negligible. The populations of the higher nP states are unknown, but we suppose that they are comparable with those of F states. Since the lifetimes of the nP states are much longer than the lifetimes of the nF states, the contributions $\Sigma A_{nP6D} N(nP)$ should not play any significant role in the rate Eq. (20). Thus, at the present experimental conditions, the steady-state rate equation for the process (1) reduces to:

$$N(6D)/\tau_{6D} = K_{6D} N^2(6P), \qquad (21)$$

which reproduces (14). Therefore we can follow the evaluation given in Sect. 2 and determine the rate coefficient K_{6D} using the expression (18). In this case, (18) can be written as:

$$K_{6D} = \frac{\nu_{3/2}}{\bar{\nu}} \frac{\beta_{3/2}\delta\nu}{(\Delta\nu)^2} \frac{I_{6D6P}}{I_{3/2}(\Delta\nu)} \frac{N(6S)}{(1+\xi)^2 N_0(6P_{3/2})} \times \frac{\int r^2\,\mathrm{d}r f(6P_{3/2}, r)}{\int r^2 \mathrm{d}r f^2(6P_{3/2}, r)}. \qquad (22)$$

The ratio of the averaged spatial distributions amounts to 1.4, the fine structure population density ratio $\xi = N_0(n_o P_{J'})/N(n_o P_J)$ is equal to 1.6, and $\bar{\nu}$ is averaged frequency of the measured EP multiplet $6D \rightarrow 6P$. Note that according to [17] the product $\tau_{6D} \times A_{6D6P}$ is nearly equal to unity.

The value for the $6D$ rate coefficient was found to be

$$K_{6D} = 4.2 \times 10^{-10}\ \mathrm{cm}^3\,\mathrm{s}^{-1}. \qquad (23)$$

The statistical error for K_{6D} is about 10%. However, including the inaccuracy of the measured densities, we estimate a total error of about 30%.

4.2 The 7D state

As in case of the $6D$ state, the influence of the radiative relaxation processes of highly lying states on the population

of the $7D$ is negligible. However, attention should be paid to the 8P state which is energetically very close to the Cs*(6P) + Cs*(5D) pair (see Fig. 4). For example, the energy of the $8P_{3/2}$ state is only 16.3 cm^{-1} higher than the energy of the Cs*($6P_{1/2}$) + Cs*($5D_{5/2}$) system. Therefore, it is expected that this state might be populated by a strong energy pooling process. On the other hand, the energy difference between the $8P$ and $7D$ states is about 300 cm^{-1}, and their mutual transfer of excitation energy by collisions with ground state Cs atoms cannot be neglected. Consequently, a correct rate equation for $7D$ state must be coupled with the rate equation for the $8P$ state:

$$\frac{d}{dt}N(7D) = -N(7D)[1/\tau_{7D} + R] + K_{7D}N(6P)N(5D) + N(8P)Q \quad (24)$$

$$\frac{d}{dt}N(8P) = -N(8P)[1/\tau_{8P} + Q] + K_{8P}N(6P)N(5D) + N(7D)R \quad (25)$$

where the collisional mixing rates for transitions $7D \rightarrow 8P$ and $8P \rightarrow 7D$ are denoted with R and Q, respectively. Taking (25) into account, the rate equation for $N(7D)$ reads as follows:

$$N(7D)\left[1/\tau_{7D} + R\left(1 - \frac{Q}{1/\tau_{8P} + Q}\right)\right] = \left[K_{7D} + K_{8P}\frac{Q}{1/\tau_{8P} + Q}\right]N(6P)\,N(5D). \quad (26)$$

The value of the cross section $\sigma_Q = 2 \times 10^{-15}$ cm^2 for the Cs($8P$) → Cs($7D$) collisional transfer by ground state cesium atoms was taken from [18] and the cross section $\sigma_R = 2.6 \times 10^{-15}$ cm^2 for the inverse process was calculated using the principle of detailed balancing. Under the present experimental conditions ($N(Cs) = 10^{16}$ cm^{-3}, $v_{rel} = 4.4 \times 10^4$ $cm\,s^{-1}$) rates Q and R are about four times smaller than the total relaxation rate of the $8P$ state ($1/\tau_{8P} = 2.8 \times 10^6$ s^{-1}). Since the total radiative relaxation rate of the $7D$ state ($1/\tau_{7D} = 1.1 \times 10^7$ s^{-1}) is much larger than the rate R, (26) can be rewritten in the approximate form:

$$N(7D)/\tau_{7D} \approx [K_{7D} + 0.25\,K_{8P}]\,N(6P)\,N(5D). \quad (27)$$

The population of the $8P$ state could not be measured here because the multiplet $8P_J \rightarrow 6D_J$ was blended by the emission of the broad Cs D_1 line. Thus, the energy pooling rate coefficients K_{7D} and K_{8P} cannot be distinguished in our experiment, and only the sum $K_{7D} + 0.25K_{8P}$ can be derived from present measurements. The population density $N_0(7D) = 1.2 \times 10^6$ cm^{-3} was measured at the number densities $N_0(6D) = 2.9 \times 10^{11}$ cm^{-3} and $N_0(5D) = 5 \times 10^{10}$ cm^{-3}. Taking into account the fact that the spatial distributions of cesium atoms in the $6P$ and $5D$ states are nearly equal (see Fig. 3b) and introducing the theoretical value $\tau_{6D} = 6.0 \times 10^{-8}$ s, we obtain from (27):

$$K_{7D} + 0.25K_{8P} \approx 1.2 \times 10^{-9}\ cm^3\,s^{-1}. \quad (28)$$

We estimate an overall experimental uncertainty of this value to be about 40%, which is mainly due to the inaccuracy of $N_0(5D)$.

4.3 The 7F state

In the case of the energy-pooling of the $7F$ state, the situation is more complicated since the collisional interaction with several neighbouring states has to be taken into account. The steady-state rate equation for $7F$ state can be written as:

$$\frac{d}{dt}N(7F) = 0 = -N(7F)[1/\tau_{7F} + \sum R_{7Fn}] + K_{7F}N^2(5D) + \sum Q_{n7F}N(n). \quad (29)$$

Here R_{7Fn} and Q_{n7F} are collisional depopulation and population rates of the $7F$ state, respectively. This equation is coupled with n other rate equations of collisionally mixed neighbouring states. Only a rough estimate for the EP rate coefficient can be made assuming that the collisional terms in (29) are negligible. In order to make the rough estimate for the value of the rate coefficient K_{7F} we applied the reduced rate Eq. (29). Using the value $\tau_{7F} = 2.4 \times 10^{-7}$ s [17] and the data displayed in Fig. 4, we obtain:

$$K_{7F} \approx N_0(7F)/\tau_{7F}N_0^2(5D) = 7 \times 10^{-10}\ cm^3\,s^{-1}. \quad (30)$$

5 Discussion and conclusions

The measured rate coefficient K_{6D} represents a sum of particular contributions regarding the fine structure of the $6P$ state. According to (19), this sum can be written as:

$$K_{6D} = \frac{\xi^2}{(1+\xi)^2}K_{6D}(\tfrac{1}{2},\tfrac{1}{2}) + \frac{\xi}{(1+\xi)^2}K_{6D}(\tfrac{1}{2},\tfrac{3}{2}) + \frac{1}{(1+\xi)^2}K_{6D}(\tfrac{3}{2},\tfrac{3}{2}). \quad (31)$$

The value of the total rate coefficient depends on the ratio of the population densities of the 6P fine structure sublevels. In our case, the ratio $\xi = N_0(6P_{1/2})/N_0(6P_{3/2}) = 1.6$ yields:

$$K_{6D} = 0.38K_{6D}(\tfrac{1}{2},\tfrac{1}{2}) + 0.24K_{6D}(\tfrac{1}{2},\tfrac{3}{2}) + 0.15K_{6D}(\tfrac{3}{2},\tfrac{3}{2}). \quad (32)$$

We were not able to distinguish the particular rate coefficients. However, following the conclusions of other experiments on EP processes in metal vapors, we can estimate the relations between particular rate coefficients in (32). As shown in [6, 8], the magnitudes of the EP rate coefficients are mainly dependent on the energy difference ΔE between the initial and final state of the collisional pair. As a result of the collisional breakdown of LS coupling, the rate coefficients seem to show no direct dependence on the electronic configurations of the initial and final states. Regarding the sign of ΔE, the rate coefficients behave in two different ways. For endothermic collisions ($\Delta E > 0$), the rate coefficients show an approximately exponential decrease ($\propto e^{-\Delta E/kT}$, $kT = 521$ cm^{-1} at $T = 750$ K) with

increasing energy difference. This is due to the fact that only a fraction of the collisional pairs has sufficient kinetic energy to produce the final state with higher excitation energy. On the other hand, in case of exothermic collisions ($\Delta E < 0$) the dependence of the rate coefficients on the absolute value of ΔE shows no systematic trend.

In our case, the term $K_{6D}(\frac{1}{2}, \frac{1}{2})$ corresponds to an endothermic EP process, for which the energy difference between final and initial state is $\Delta E \approx -260\,\mathrm{cm}^{-1}$. The $K_{6D}(\frac{1}{2}, \frac{3}{2})$ and $K_{6D}(\frac{3}{2}, \frac{3}{2})$ correspond to the exothermic *EP* processes with energy differences $+290\,\mathrm{cm}^{-1}$ and $+850\,\mathrm{cm}^{-1}$, respectively. Regarding the energy differences, one can expect that $K_{6D}(\frac{3}{2}, \frac{3}{2})$ is much smaller than the other two cross rate coefficients. Thus, the expression (32) can be written in approximate form:

$$K_{6D} \approx 0.38 K_{6D}(\tfrac{1}{2}, \tfrac{1}{2}) + 0.24 K_{6D}(\tfrac{1}{2}, \tfrac{3}{2}). \tag{33}$$

In order to distinguish the rate coefficients $K_{6D}(\frac{1}{2}, \frac{1}{2})$ and $K_{6D}(\frac{1}{2}, \frac{3}{2})$, the experiment should be performed with selective excitation of the $6P$ finite-structure levels.

To compare our present results with results of other groups, we calculated the EP cross sections σ_i related to the measured rate coefficients K_i by $\sigma_i = K_i/\bar{v}$. With $\bar{v} = 4.4 \times 10^4\,\mathrm{cm\,s}^{-1}$, the calculated cross sections are:

$$\sigma_{6D} = 9.5 \times 10^{-15}\,\mathrm{cm}^2, \tag{34}$$

$$\sigma_{7D} + 0.25\sigma_{8P} \approx 2.8 \times 10^{-14}\,\mathrm{cm}^2, \tag{35}$$

and

$$\sigma_{7F} \approx 1.5 \times 10^{-14}\,\mathrm{cm}^2. \tag{36}$$

In an experimental investigation [19] related to ours, the inverse process of (1), i.e. the collisional process $\mathrm{Cs}^{**}(6D_{3/2}) + \mathrm{Cs}(6S) \rightarrow \mathrm{Cs}^{*}(6P) + \mathrm{Cs}^{*}(6P)$ had been investigated. At nearly the same conditions as in our experiment, the measured cross section was $\sigma^{\mathrm{inv}} = 1.5 \times 10^{-14}$ cm^2. Neglecting $\sigma_{6D}(\frac{3}{2}, \frac{3}{2})$ and applying the principle of detailed balancing, one can easily find that σ^{inv} is a linear combination of $\sigma_{6D}(\frac{1}{2}, \frac{1}{2})$ and $\sigma_{6D}(\frac{1}{2}, \frac{3}{2})$:

$$\sigma^{\mathrm{inv}} = 0.61\sigma_{6D}(\tfrac{1}{2}, \tfrac{1}{2}) + 0.25\sigma_{6D}(\tfrac{1}{2}, \tfrac{3}{2}). \tag{37}$$

An exact correlation between our result for the cross section of the process (1) and the cross section reported in [19] for the inverse process cannot be made. However, by comparison of (33) and (37), it is obvious that these results are in qualitative agreement.

As mentioned in the introduction, a theoretical study of the EP process (1) has been reported in [10]. Taking into account exchange and dipole-dipole interaction, the authors of [10] calculated the cross section for the reaction (1). They concluded that the main channel for the reaction (1) is related to the $6P_{1/2} + 6P_{3/2}$ configuration and the obtained cross section was estimated to be between 1.5×10^{-15} cm^2 and 2.0×10^{-14} cm^2.

Our results fit well into the set of measured EP cross sections for homonuclear and heteronuclear alkali atoms [6]. The investigated EP processes are among the strongest reactions of that type in alkali vapors. The magnitude of the corresponding cross sections indicates that the investigated EP reactions in cesium occur at interatomic distances larger than 1 nm, i.e. in the region where electrostatic multipole interaction is dominant. Therefore, cesium is an ideal system for the further theoretical consideration of EP processes.

We acknowledge gratefully financial support by the Ministry of Science (Republic of Croatia) and by the Deutsche Forschungsgemeinschaft (project no. Ni 185/17). The authors thank D. Veza for the assistance.

References

1. Klyucharev, A.N., Lazarenko, A.V.: Opt. Spektrosk. **32**, 1063 (1972) (Opt. Spectrosc. (USSR) **32**, 576 (1972))
2. Allegrini, M., Alzetta, G., Kopystynska, K., Moi, L., Orriols, G.: Opt. Commun. **19**, 96 (1976)
3. Huennekens, J., Gallagher, A.: Phys. Rev. A**27**, 771 (1983)
4. Allegrini, M., Bicchi, P., Moi, L.: Phys. Rev. A**28**, 1338 (1983)
5. Barbier, L., Cheret, M.: J. Phys. B**16**, 3213 (1983)
6. Gabbannini, C., Gozzini, S., Squadrito, G., Allegrini, M., Moi, L.: Phys. Rev. A**39**, 6148 (1989)
7. Gabbannini, C., Biagini, M., Gozzini, S., Lucchesini, A., Kopystynska, A., Moi, L.: J. Quant. Spectrosc. Radiat. Transfer. **47**, 103 (1992)
8. Werij, H.G.C., Harris, M., Cooper, J., Gallagher, A.: Phys. Rev. A**43**, 2237 (1991)
9. Neuman, J.A., Gallagher, A.: Phys. Rev. A**50**, 1292 (1994)
10. Borodin, M.V., Komarov, I.V.: Opt. Spectrosc. (USSR) **36**, 145 (1974)
11. Sobel'man I.I., Vainshtein, L.A., Yukov, E.A.: Excitation of atoms and broadening of spectral lines. Berlin, Heidelberg, New York: Springer 1981
12. Movre, M., Pichler, G.: J. Phys. B**13**, 697 (1980)
13. Horvatic, V., Movre, M., Beuc, R., Vadla, C.: J. Phys. B**26**, 3679 (1993)
14. Vadla, C., Niemax, K., Horvatic, V., Beuc, R.: Z. Phys. D**34**, 171 (1995)
15. Nesmeyanov, A.N.: Vapor pressure of the elements. New York: Academic Press 1963
16. Keramati, B., Masters, M., Huennekens, J.: Phys. Rev. A**38**, 4518 (1988)
17. Hansen, W.: J. Phys. B**17**, 4833 (1984)
18. Pimbert, M.: J. Phys. **33**, 331 (1972)
19. Yabuzaki, T., Tam, A.C., Hou, M., Happer, W., Curry, S.H.: Opt. Commun. **24**, 305 (1978)